Metal–Metal Interactions in Dinuclear (triphos)Cobalt Complexes Exhibiting Mixed Valency

Katja Heinze,[a] Gottfried Huttner,*[a] and Olaf Walter[a]

In memoriam Dr. L. Zsolnai

Keywords: Tripodal ligands / Cobalt / Bridging ligands / Mixed-valence compounds

The spectroscopic and electrochemical properties of a series of dinuclear mixed-valence complexes containing two (triphos)Co units are reported: $[(triphos)Co(L)Co(triphos)]^+$ (L = $C_6O_4X_2$; X = H, Cl, Br, I, Me: **2a–e$^+$**; L = $C_{14}H_4O_4Me_2$: **4$^+$**). Complexes **2a–e$^+$** are bridged by tetraoxybenzene ligands and exhibit very strong metal–metal interaction leading to delocalized class-III behaviour while in **4$^+$** the extended tetraoxoanthracence bridging ligand leads to a partial electron localization. Additionally, the different oxidation behaviour of the parent dicationic complexes **1a–e^{2+}** and **3^{2+}** have been investigated and are explained on the basis of a qualitative MO model.

Introduction

In the frame of a general study of magnetic[1][2] and electronic[3] interactions between two cobalt centres connected through a bridging ligand we have been interested in the investigation of complexes of the type $[(triphos)Co(L)Co(triphos)]^{n+}$. The tridentate terminal ligand triphos [1,1,1-tris(diphenylphosphanylmethyl)ethane] induces a five-fold coordination around each cobalt centre providing two free *cis* coordination sites[4–6] and thus allowing a bis(bidentate) coordination mode of the bridging ligand L within the dinuclear complex. The phosphorus donor set usually splits the metal d orbitals such that low-spin configurations (d^6-Co^{III}; d^7-Co^{II}) with zero or one unpaired electron, respectively, are obtained.[4][5] Antiferromagnetic exchange coupling is observed between the unpaired electrons of two $[(triphos)Co^{II}]$ entities in the complexes $[(triphos)Co(L)Co(triphos)]^{2+}$ with L = di-μ-X (X = Cl,[7][8] Br,[7] OH,[7] NH_2,[9] SMe[10]), 1,4,5,8-tetraoxonaphthalene, 1,4,9,10-tetraoxoanthracene,[1] fumarate and terephthalate.[2] Strong metal−bridging ligand interaction occurs within the dinuclear $[(triphos)Co^{III}]$ complexes $[(triphos)Co(L)Co(triphos)]^{2+}$ with L = 3,6-disubstituted 1,2,4,5-tetraoxybenzenes resulting in unusually intense, low-energy LMCT absorption bands.[3] In all cases the π system of the bridge proved to be essential for the interaction. In the latter complexes a further manifestation of the interaction is the separation of the two metal-centered reduction potentials which is due to the efficient overlap of the metal d(π) orbitals with the π orbitals of the bridging ligand.

We therefore attempted to prepare, isolate and characterize cationic mixed-valence complexes of the type $[(triphos)Co(L)Co(triphos)]^+$ with L = 3,6-disubstituted 1,2,4,5-tetraoxybenzenes in order to address the question of electron delocalization and electron transfer within the dinuclear unit. As the length of the bridging ligand has a remarkable influence on the communication between metal centres, analogous complexes with the extended bridging ligand 1,2,6,7-tetraoxy-9,10-dimethylanthracene are also reported.

[a] Department of Inorganic Chemistry, University of Heidelberg
Im Neuenheimer Feld 270, D-69120 Heidelberg, Germany
Fax: (internat.) + 49(0)6221/545707

Results and Discussion

Preparation of Complexes 1a−e^{2+}, 2a−e$^+$; Thermodynamic Stability and Reactivity of 2a−e$^+$

The complexes $[(triphos)Co(C_6O_4X_2)Co(triphos)]^{2+}$ (X = H, Cl, Br, I, Me), **1a−e^{2+}**, were prepared according to the literature.[3] Their CV data have already been reported but are repeated here for completeness (Table 1). The exceptionally large separation of the two reversible reduction steps shows that the mixed-valence species are thermodynamically stable towards disproportionation into the neutral and dicationic complexes. The green dicationic complexes can be reduced with one equivalent of cobaltocene to the blue cationic complexes **2a−e$^+$** (Figure 1; equation 1) which can be characterized in solution by spectroscopic methods. Reoxidation is possible by reaction with ferrocenium tetrafluoroborate (70−80% recovery).

All attempts to isolate **2a−e$^+$** as pure and crystalline materials failed as the complexes **2a−e$^+$** rapidly decompose on removing the solvent. Furthermore the mixed-valence complexes are highly reactive towards dioxygen leading to decomposition of the complexes (rapid colour change to red-brown yielding the free bridging ligand and phosphane oxides[11]). The reduction of **1a−e^{2+}** to **2a−e$^+$** was also carried out by the reaction with primary and secondary sodium alkoxides (NaOR; R = Me, Et, *i*Pr, CH_2Ph, allyl) yielding the corresponding aldehydes and ketones, respectively (isolated as their 2,4-dinitrophenylhydrazones). No carboxylic acids were detected in the reaction mixture. Ti-

  1434−1948/99/0404−0593v $ 17.50+.50/0

Table 1. Spectroscopic data of **2a−e**$^+$

X =	H (**2a**$^+$)	Cl (**2b**$^+$)	Br (**2c**$^+$)	I (**2d**$^+$)	Me (**2e**$^+$)
UV/Vis[a]					
λ_1 [nm] (ε [M^{-1} cm^{-1}])	300 (25510, sh)	305 (21680, sh)	322 (13750,sh)	303 (20030, sh)	300 (25860, sh)
λ_2 [nm] (ε [M^{-1} cm^{-1}])	394 (5630, sh)	392 (5580, sh)	–	–	394 (6390, sh)
λ_3 [nm] (ε [M^{-1} cm^{-1}])	450 (4450, sh)	447 (4530, sh)	422 (3870, sh)	405 (5300, sh)	456 (4630, sh)
λ_4 [nm] (ε [M^{-1} cm^{-1}])	–	658 (11540, sh)	664 (9560, sh)	658 (10860, sh)	–
λ_5 [nm] (ε [M^{-1} cm^{-1}])	692 (21380)	720 (15240)	720 (12230)	717 (12360)	689 (18800)
λ_6 [nm] (ε [M^{-1} cm^{-1}])	843 (7890, sh)	861 (7050, sh)	855 (5630, sh)	872 (5170, sh)	835 (7660, sh)
Isosbest. point [nm][b]	866	923	923	914	832
CV ($E_{1/2}$)[c]	−105, −1170	+10, −1000	+5, −1000	0, −995	−165, −1250
K_C (CV, 298 K)	11 × 10^{17}	1.2 × 10^{17}	1.0 × 10^{17}	0.6 × 10^{17}	22 × 10^{17}
EPR					
g_{av} (298 K)[a]	2.11	2.11	2.11	2.11	2.11
A_1, A_2 [G] (298 K)	–	–	–	–	40, 29
g_x, g_y, g_z (100 K)[d]	2.21, ?, 2.00	2.21, ?, 2.00	2.21, ?, 2.00	2.21, ?, 2.00	2.21,2.06,2.00[e]
A_x, A_y, A_z (100 K)	40, ?, 34	40, ?, 34	40, ?, 34	40, ?, 34	40, 40, 34

[a] In CH_2Cl_2. – [b] Titration experiment with *i*PrONa in CH_2Cl_2/*i*PrOH (3:1). – [c] In CH_3CN. – [d] In THF/CH_2Cl_2 (2:1). – [e] Simulation.

equation 1

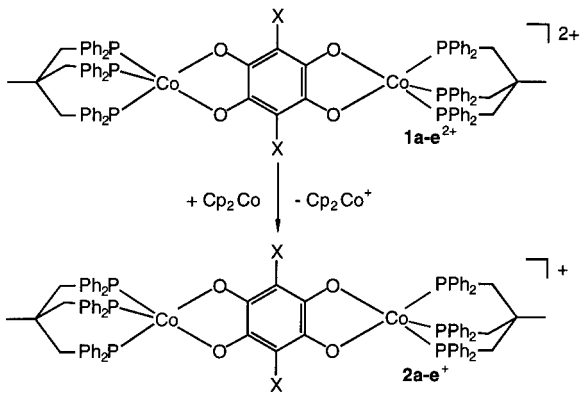

equation 2

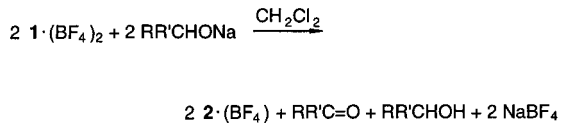

Figure 1. Reduction of **1a−e**$^{2+}$ to **2a−e**$^+$

trations with NaO*i*Pr, monitored by UV/Vis spectroscopy, showed clearly that one equivalent of base is necessary for complete conversion of **1a−e**$^{2+}$ to **2a−e**$^+$ (Table 1). The UV/Vis spectra obtained for the titration of **1c**$^{2+}$ with NaO*i*Pr are shown in Figure 2 as an example.

The intensity of the characteristic LMCT absorption band of **1c**$^{2+}$ at 1195 nm decreases with increasing base concentration, and simultaneously the band pattern of the cationic complex **2c**$^+$ emerges. Three isosbestic points are visible (304, 434 and 923 nm) which show that no UV/Vis-detectable intermediates are present. The net reaction can therefore be written as shown in Figure 1 (equation 2). These solutions are somewhat more stable than solutions of

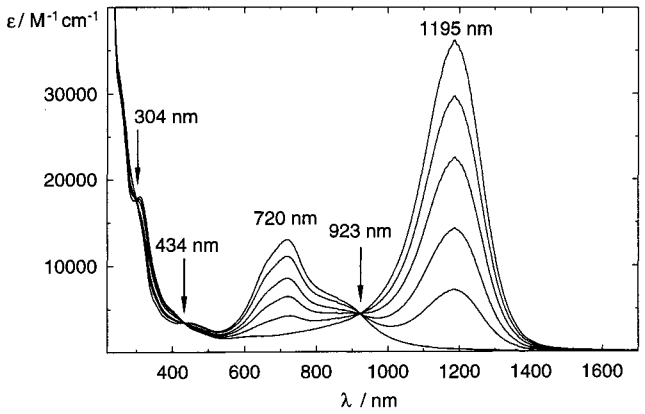

Figure 2. UV/Vis spectra during the titration of **1c**$^{2+}$ with NaO*i*Pr

2a−e$^+$ in pure CH_2Cl_2 and/or THF as long as an excess alcoholate is present.

Spectroscopic Properties of 2a−e$^+$

The isotropic EPR spectra of **2a−e**$^+$ in CH_2Cl_2 at 295 K show a broad, poorly resolved signal at *g* factors of around 2.11 (Table 1). The *g* factor and the width (half width at full height ca. 140 G) of the signal exclude the possibility of a significant spin density located on the bridging ligand. In a THF/CH_2Cl_2 matrix at 100 K the EPR spectrum exhibits a complex line pattern centered around $g = 2.10$. Figure 3 (left) shows the EPR spectrum of **2e**$^+$ as an example.

A 3 × 8 signal pattern would be expected if the unpaired electron were localized at one cobalt centre ($I_{Co} = {}^7/_2$), whereas a coupling with two equivalent cobalt centres should result in a 3 × 15 line pattern. Attempts to simulate the obtained spectra with a coupling to one metal centre failed; on the other hand a satisfactory approximation of the spectra was possible with the assumption of a coupling with two metal centres (Figure 3, right). This leads to the conclusion that the unpaired electron is delocalized over both metal centres, at least on the EPR time scale (10^{-9} s).

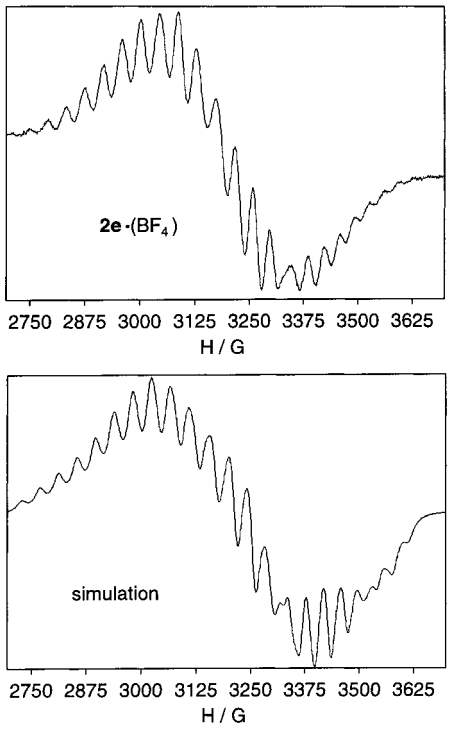

Figure 3. EPR spectrum of $\mathbf{2e}^+$ in THF/CH_2Cl_2 at 100 K and simulated spectrum

The obtained hyperfine coupling constants of $A_x \approx 40$ G, $A_y \approx 40$ G and $A_z \approx 34$ G further corroborate this interpretation. The coupling is significantly smaller than that found in the related mononuclear Co^{II} complexes [(triphos)-Co(L)] (L = substituted catecholate) with the unpaired electron inevitably localized on one metal centre ($A_x \approx 68-74$ G, $A_y \approx 58-60$ G and $A_z \approx 48-53$ G[12][13]).

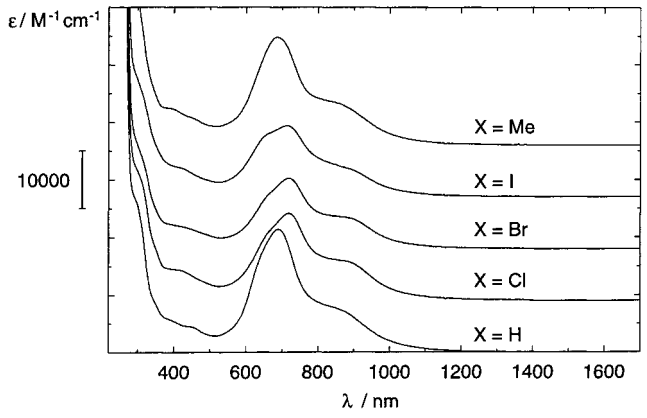

Figure 4. UV/Vis spectra of $\mathbf{2a-e}^+$

In accord with this interpretation of a delocalized system no absorption band which could be assigned to an intervalence transition could be detected up to 1700 nm in the UV/Vis/NIR spectra (Figure 4). In the visible part of the spectra a three-band pattern is observed (Table 1; $\lambda_4-\lambda_6$). The energy of the band maxima depends slightly on the substituents at the central bridge: Halides induce a red shift ($\mathbf{2a-d}^+$), alkyl residues a blue shift ($\mathbf{2e}^+$). This trend was also observed for the parent compounds $\mathbf{1a-e}^{2+}$.[3] The low-energy shoulder λ_6 has a half width at full height of only ca. 1630 cm^{-1} which is more than three times smaller than expected for a partly localized class-II system according to the Hush theory (5150−5260 cm^{-1}[14][15]). This transition might therefore better be described as a $\pi-\pi^*$ transition between delocalized states. Based on the CV, EPR, and UV/Vis data we therefore formulate the complex cations $\mathbf{2a-e}^+$ as delocalized class-III systems.

Crystal Structure of $(\mathbf{2b})_2\cdot(CoCl_4)$

Crystals of the complex salt $(\mathbf{2b})_2 \cdot (CoCl_4)$ were obtained as described in the Experimental Section. $(\mathbf{2b})_2 \cdot (CoCl_4)$ crystallizes in the tetragonal space group *P*4/*n*. The cation possesses crystallographic inversion symmetry, the $CoCl_4^{2-}$ counterion crystallographic S_4 symmetry. The results of the structural analysis are presented in Figure 5 and Table 2. In addition selected bond lengths and angles of the parent dicationic complex $(\mathbf{1b}) \cdot (BF_4)_2$[3] are shown for comparison.

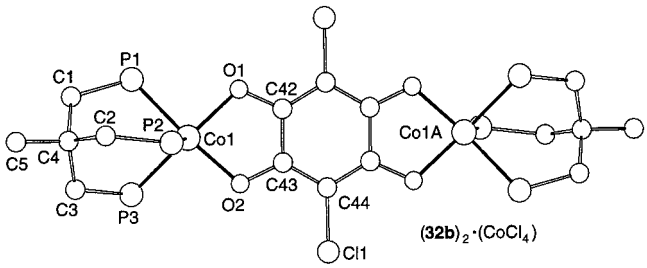

Figure 5. View of the structure of $\mathbf{2b}^+$; phenyl rings of the triphos ligand are omitted for clarity reasons

Neither a ligand dissociation nor a significant distortion of the coordination geometry relative to the structure of $\mathbf{1b}^{2+}$ is observed (maximum angle deviation X−Co−Y is observed for P3−Co1−O2 with 4.4°). Likewise the intraligand bond lengths (C−C, C−O, C−Cl) remain identical within the 2σ limit. Significant changes of the bond lengths are observed for the Co−O and Co−P bonds. The Co1−P2 (Δx = 0.073 Å) and the Co1−O1,2 bonds (Δx = 0.045, 0.053 Å) especially are elongated. As mainly bond lengths and only to a minor extent bond angles are affected by the additional electron the Franck−Condon barrier for the electron transfer can be estimated via $E_{in} = {}^1/_2\, N \Sigma\, k_i\, (\Delta x_i/2)^2$[16] [with k(Co−P) = 200 N m^{-1}; k(Co−O) = 440 N m^{-1}] resulting in about 2.5 kJ mol^{-1} per cobalt centre (i.e. 5 kJ mol^{-1} per complex). For the redox couple $[Co(tacn)_2]^{2+/3+}$ (tacn = 1,4,7-triazacyclononane) E_{in} is calculated as 25 kJ mol^{-1} [k(Co−N) = 170 N m^{-1}; Δx = 0.181 Å].[17] The very low activation barrier for the self-exchange reaction is due to the extremely small changes of the cobalt−ligand bond lengths Δx which might be the result of two effects: first the fact that the electron is delocalized over two metal centres and second that the cobalt centres retain their low-spin state as opposed to the $[Co(tacn)_2]^{2+/3+}$ case (hs-Co^{II}/ls-Co^{III}).

Table 2. Selected bond lengths[a] [Å] and angles[a] [°] for (**1b**) · $(BF_4)_2$ and $(\mathbf{2b})_2$ · $(CoCl_4)$

	1b · $(BF_4)_2$	$(\mathbf{2b})_2$ · $(CoCl_4)$		**1b** · $(BF_4)_2$	$(\mathbf{2b})_2$ · $(CoCl_4)$
Co1−O1	1.873(3)	1.918(5)	O1−Co1−O2	84.2(1)	82.7(2)
Co1−O2	1.881(3)	1.934(5)	C42−O1−Co1	113.6(3)	113.2(4)
Co1−P1	2.200(1)	2.220(2)	C43−O2−Co1	113.0(3)	113.6(4)
Co1−P2	2.178(1)	2.251(2)	O1−C42−C43	114.2(4)	114.4(6)
Co1−P3	2.204(1)	2.225(2)	O2−C43−C42	114.2(4)	114.8(6)
O1−C42	1.311(5)	1.311(8)	P1−Co1−P2	92.29(5)	91.62(9)
O2−C43	1.321(5)	1.311(8)	P1−Co1−P3	90.77(5)	88.59(8)
C42−C43	1.442(6)	1.45(1)	P2−Co1−P3	89.96(5)	91.63(8)
C43−C44	1.385(7)	1.40(1)	P1−Co1−O1	89.8(1)	90.5(2)
C42−C44A	1.390(5)	1.39(1)	P1−Co1−O2	161.7(1)	164.6(2)
C44−Cl1	1.737(5)	1.743(7)	P2−Co1−O1	111.5(1)	108.8(2)
Co1···Co1A	7.56	7.67	P2−Co1−O2	106.0(1)	103.6(2)
			P3−Co1−O1	158.5(1)	159.6(2)
			P3−Co1−O2	88.6(1)	93.0(2)
Co2−Cl2	−	2.301(2)	Cl2−Co2−Cl2A	−	109.60(8)
τ_1[b]	13.6	13.4	φ_1[b]	12.7	5.9
τ_2	15.1	7.9	φ_2	44.4	45.6
τ_3	16.2	16.0	φ_3	15.4	13.5
			φ_4	46.8	33.2
			φ_5	17.6	25.6
			φ_6	16.6	11.0

[a] Estimated standard deviations of the least significant figures are given in parentheses. − [b] The torsion angles τ_x are defined as follows: C4−C_x−P_x−Co (x = 1−3). The torsional arrangement of the six phenyl groups (φ_1−φ_6) is defined with respect to auxiliary vectors Hz_x−P_x (Hz_x is a dummy atom above P_x orthogonal to the plane spanned by the three phosphorus atoms) (x = 1−3): Hz_x−P_x−C_{ipso}−C_{ortho}.

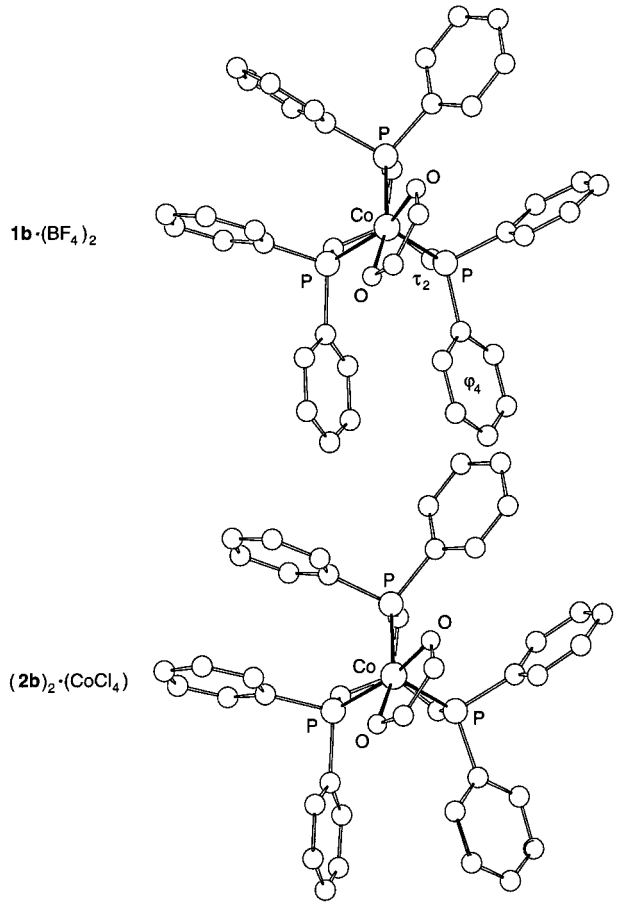

Figure 6. View of one (triphos)Co(O_2C_2) fragment of $\mathbf{1b}^{2+}$ and $\mathbf{2b}^{+}$[3] perpendicular to the plane spanned by the three phosphorus atoms

The conformation of the triphos ligand in the complex cations $\mathbf{1b}^{2+}$ and $\mathbf{2b}^{+}$ as decribed by the torsion angles of the chelate cage τ_{1-3} and the rotational position of the six phenyl rings φ_{1-6}[6] is shown in Figure 6 and Table 2. The only significant changes involve the backbone torsion angle τ_2 ($\Delta\tau_2 \approx 7°$) and the orientation of the fourth phenyl ring ($\Delta\varphi_4 \approx 14°$) both associated with the phosphorus atom P2.

In summary the structural data show that the additional electron in $\mathbf{2b}^{+}$ is neither localized on the bridging ligand nor on the triphos ligand, but on the metal centres. Of course, the X-ray structural analysis does not allow a decision between a localized or delocalized electronic description.

MO Calculations

The results of a molecular orbital calculation on the model compound $[\{(PH_3)_3Co\}_2(C_6H_2O_4)]^{2+}$ by the INDO method are presented in Figure 7,[18] which shows the relative energies and symmetries of the frontier orbitals. Here it suffices to note that in accordance with the EPR results the additional electron occupies a (68%) molecular orbital of b_u symmetry (C_{2h}) centered mainly on both metal atoms and that a filled ligand-centered (99% ligand) MO of b_g symmetry lies *below* the essentially ligand-centered MO of a_g symmetry (70% ligand).

Preparation of Complexes 3^{2+}, 4^{+}, 5^{3+}

The dicationic complex **3** · $(PF_6)_2$ may be obtained from $CoCl_2$, triphos, the bridging ligand 2,3,6,7-tetrahydroxy-9,10-dimethylanthracene and $NaPF_6$ as an analytically pure

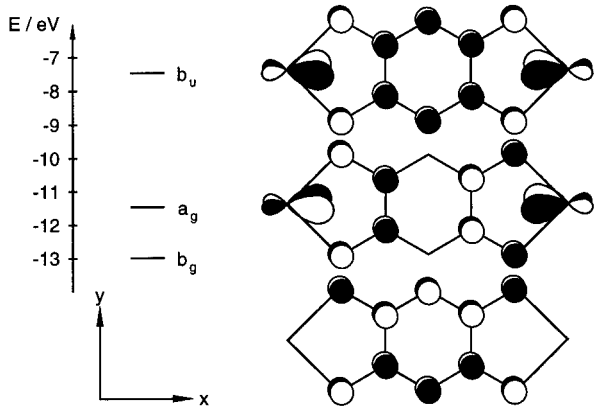

Figure 7. Orbital splitting and orbital symmetry of the model complex $[\{(PH_3)_3Co\}_2(C_6H_2O_4)]^{2+}$; the symmetry labels for the orbitals assume C_{2h} symmetry; the x axis is the Co−Co axis, and the z axis is perpendicular to the plane of the bridging ligand

blue powder. The FAB mass spectrum shows a typical fragmentation pattern[1−3] of dinuclear dicationic (triphos)cobalt complexes (see Experimental Section). The ^{1}H-NMR spectrum of **3** · $(PF_6)_2$ in CD_2Cl_2 shows signals for the CH_3, CH_2 and CH groups of the triphos ligand and signals for the CH and CH_3 groups of the bridging ligand in the correct intensity ratio. The phosphorus atoms of the triphos ligand give rise to a singlet at $\delta = 31.1$ in the ^{31}P-NMR spectrum. The signal of the ^{31}P nucleus of the hexafluorophosphate counterion is observed at $\delta = -144.2$ with the correct intensity ratio[19] of P(PF_6)/P(triphos) = 1:3. Due to the low solubility of **3** · $(PF_6)_2$ no ^{13}C-NMR spectrum could be obtained.

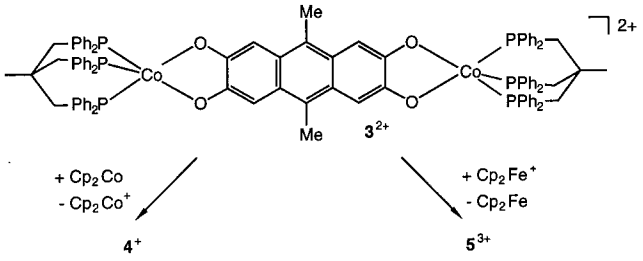

Figure 8. Synthesis of 4^+ and 5^{3+}

The dicationic complex 3^{2+} can be reduced in two reversible steps at −170 mV (Figure 9; 1) and −355 mV (Figure 9; 2), reversibly oxidized at +335 mV (Figure 9; 3) and irreversibly oxidized at $E_p \approx +935$ mV (vs. SCE). The reversible character of both reduction steps and the first oxidation wave precludes any significant structural rearrangement during the redox processes, i.e. all species 3^{2+}, 4^+ and 5^{3+} can be described by the same structure. The reduction to the mixed-valence complex 4^+ can be accomplished with cobaltocene; the oxidation to the trication 5^{3+} with ferrocenium tetrafluoroborate (Figure 8). With the separation of the two reduction potentials of 185 mV the conproportionation constant K_C for 4^+ is estimated to be 1.3×10^3 which is 15 orders of magnitude smaller than K_C of the complex $2e^+$.

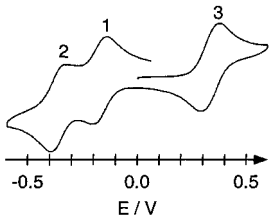

Figure 9. Cyclic voltammogram of **3** · $(PF_6)_2$ in CH_3CN

The UV/Vis spectrum of 3^{2+} (Figure 10, Table 3) shows two intense LMCT bands at 610 and 909 nm and intraligand absorptions around 400 nm as well as a weak absorption at 1250 nm which might have also LMCT character (vide supra).

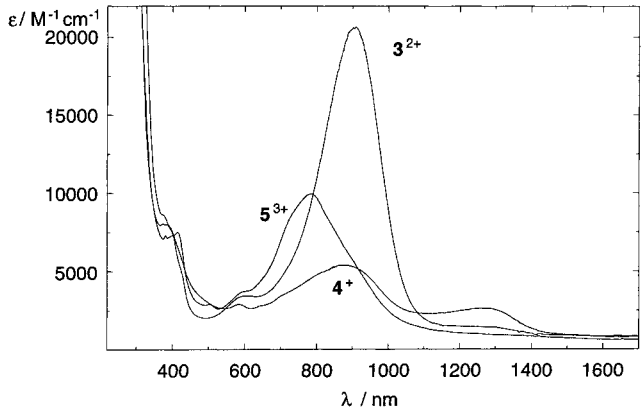

Figure 10. UV/Vis spectra of 3^{2+}, 4^+ and 5^{3+}

Spectroscopic Properties of 4^+

Reduction of 3^{2+} to 4^+ with one equivalent of cobaltocene leads to an orange-brown solution. The UV/Vis spectrum is depicted in Figure 10. Analogous to the mixed-valence complexes **2a**−**e**$^+$ it shows a three-band pattern in the Vis/NIR region. The low-energy absorption is red shifted compared to the corresponding bands of **2a**−**e**$^+$ (Tables 1 and 3). This absorption band might be a candidate for an intervalence transition although its half width at full height (1785 cm^{-1}) is lower than expected for a class-II mixed-valence system according to the Hush theory.[14][15] The characteristic features of this absorption band are quite similar to those of the well-known Creutz−Taube ion.[14] Therefore 4^+ might well be considered a borderline case between a class-II and a class-III system[20] which is also in accord with the thermodynamic data obtained by cyclic voltammetry (Table 3).

Spectroscopic Properties of 5^{3+}

One-electron oxidation of 3^{2+} gives the green tricationic complex 5^{3+}. The stability of 5^{3+} towards dispro-

Table 3. Spectroscopic data of $\mathbf{3}^{2+}$, $\mathbf{4}^{+}$ and $\mathbf{5}^{3+}$

	$\mathbf{4}^{+}$	$\mathbf{3}^{2+}$	$\mathbf{5}^{3+}$
Colour	orange-brown	blue	green
UV/Vis[a]	374 (8060) 584 (2890) 876 (5410)	376 (9450) 404 (6360, sh) 610	382 (7320) 414 (7510) 504 (2880)
λ [nm] (ε [M^{-1} cm^{-1}])	1271 (2640)	(3540) 909 (19140)	598 (3720, sh) 784 (9950)
K_C (CV, 298 K)[b]	1.3×10^3	3.4×10^8	(1.4×10^{10})
EPR (298 K)[a]	silent	diamagnetic	$g = 2.0056$

[a] In CH_2Cl_2. – [b] In CH_3CN.

portionation can only be estimated as the oxidation of $\mathbf{5}^{3+}$ is not reversible. Using the peak potential E_p instead of $E_{1/2\ KC}$ can be estimated to be of the order of 10^8. The UV/Vis spectrum of $\mathbf{5}^{3+}$ is similar to that of $\mathbf{3}^{2+}$ (Figure 10); the charge-transfer bands at 598 and 784 nm are shifted to higher energy and are less intense compared to those of $\mathbf{3}^{2+}$ (Tables 1 and 3). The isotropic EPR spectrum of a CH_2Cl_2 solution of $\mathbf{5}^{3+}$ is shown in Figure 11. The sharp signal centered at $g = 2.0056$ is without observable hyperfine splitting (half width at full height 24 G). This signal is characteristic for organic radicals, showing that the organic part of the dinuclear complex is oxidized.

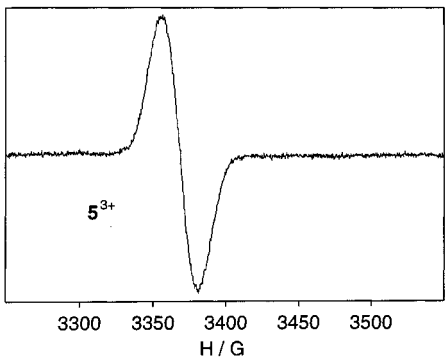

Figure 11. EPR spectrum of $\mathbf{5}^{3+}$ in CH_2Cl_2 at 295 K

MO Calculations

The frontier orbitals of the model complex $[\{(PH_3)_3Co\}_2(C_{14}H_6O_4)]^{2+}$ calculated by the INDO method are shown in Figure 12. As in the case of the complexes $\mathbf{1}^{2+}$ (Figure 7) interaction of the metal fragments with π orbitals of the bridging ligand results in two Co−O π-bonding MOs with large ligand character (b_u: 85%, not shown and a_g: 81% ligand, Figure 12) and in two Co−O π-antibonding MOs which are essentially metal-localized (b_u: 63%, and a_g: 57% metal, not shown, Figure 12). A non-bonding ligand-centered filled π orbital (b_g: 99% ligand) is located energetically between these occupied and empty orbitals. By analogy with the complexes $\mathbf{1a-e}^{2+}$ the intense absorption band at 909 nm can be assigned to the $a_g \rightarrow b_u$ transition and the additional low-energy absorption at 1250 nm to a $b_g \rightarrow b_u$ LMCT transition.

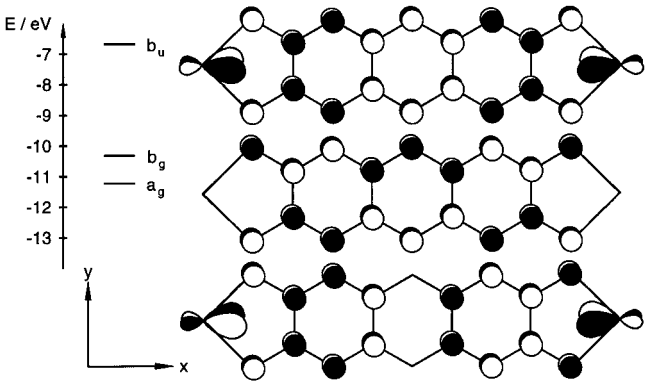

Figure 12. Orbital splitting and orbital symmetry of the model complex $[\{(PH_3)_3Co\}_2(C_{14}H_6O_4)]^{2+}$; the symmetry labels for the orbitals assume C_{2h} symmetry; the x axis is the Co−Co axis, and the z axis is perpendicular to the plane of the bridging ligand

With this MO scheme in mind the interpretation of the redox processes is straightforward: Reduction occurs, as in the case of the redox couple $\mathbf{1}^{2+}/\mathbf{2}^{+}$, at the metal centres leading to mixed-valence species. A reversible oxidation of $\mathbf{3}^{2+}$ which is not observed for $\mathbf{1}^{2+}$, is possible due to the energetically higher Co−O non-bonding ligand-centered b_g molecular orbital. For the complexes $\mathbf{1}^{2+}$ the HOMO of the complexes is Co−O π bonding (Figure 7) and oxidation would weaken the Co−O π bonds.

Concluding Remarks

The mixed-valence (triphos)cobalt complexes $\mathbf{2a-e}^{+}$ with a benzoic system as a bridging ligand ($d_{Co-Co} \approx 7.7$ Å) are shown to belong to class III of the Robin−Day classification, i.e. exhibit complete electron delocalization. In complex $\mathbf{4}^{+}$ with an extended bridging ligand of the anthracence type ($d_{Co-Co} \approx 13$ Å) the delocalization decreases towards a borderline class-II/class-III case. The assignments are corroborated by spectroscopic and theoretical means. In addition, the unexpected oxidation of the dicationic complex $\mathbf{3}^{2+}$ to $\mathbf{5}^{3+}$ leading to a ligand-centered radical is also interpreted in terms of the MO level ordering.

Experimental Section

Computational Details: Calculations were performed with an Apple Macintosh IIfx using the CACHe/ZINDO program Version 3.6 (M. C. Zerner 1990−1994) with INDO/1 parameters. Orbital energies were obtained from an SCF calculation. The geometry of the molecules was idealized to a square-pyramidal polyhedron around the metal centre and a planar bridging ligand. The triphos ligand was replaced by three isoelectronic PH_3 groups. Distances and angles were as follows: Co−P_{eq} 2.14 Å, Co−P_{ax} 2.22 Å, Co−O 1.89 Å, P−H 1.41 Å, O−Co−O 82.8°, P−Co−P 87.5°.

General Methods: Unless noted otherwise all manipulations were carried out under an inert gas by means of standard Schlenk techniques. All solvents were dried by standard methods and distilled under inert gas. − NMR: Bruker AC 200 at 200.13 MHz (^{1}H), 50.323 MHz (^{31}P). − IR: Bruker FTIR IFS-66, as CsI disks. − UV/Vis/NIR: Perkin Elmer Lambda 19. − MS: Finnigan MAT 8230. − EPR: Bruker ESP 300 E, X-band, standard cavity ER 4102, temperature control unit Eurotherm B-VT 2000, external standard diphenylpicrylhydrazyl (DPPH). − Elemental analyses: Microanalytical Laboratory of the Organisch-Chemisches Institut, University of Heidelberg. − Melting points: Gallenkamp MFB-595 010, melting points are not corrected. − Cyclic voltammetry: Metrohm "Universal Meß- und Titriergefäß", Metrohm GC electrode RDE 628, platinum electrode, SCE electrode, Princeton Applied Research potentiostat Model 273, 10^{-3} M in 0.1 M nBu$_4$NPF$_6$/CH_3CN. − Chemicals: 1,1,1-tris(diphenylphosphanylmethyl)-ethane, $CH_3C(CH_2PPh_2)_3$,[21] **1a−e** · $(BF_4)_2$,[3] 2,3,6,7-tetrahydroxy-9,10-dimethylanthracene,[22] (triphos)CoCl.[8,23,24]

Crystallographic Structure Determination: The measurement was carried out with a Siemens P4 (Nicolet Syntex) R3m/v four-circle diffractometer with graphite-monochromated Mo-K_α radiation. All calculations were performed using the SHELXT PLUS software package. The structure was solved by direct methods with the SHELXS-86 program and refined with the SHELX93 program.[25] Graphics were prepared using XPMA and ZORTEP.[26] An absorption correction (ψ scan, Δψ = 10°) was applied to all data. Atomic coordinates and anisotropic thermal parameters of the non-hydrogen atoms were refined by a full-matrix least-squares calculation. $C_{88}H_{78}Cl_4Co_{2.5}P_6O_4$ (· 0.8 Et_2O, 0.5 THF), M = 1674.6 g mol^{-1}, crystal dimensions 0.30 × 0.35 × 0.25 mm, tetragonal, Z = 4, space group $P4/n$ (no. 85), a = 23.773(6) Å, b = 23.776(6) Å, c = 16.301(4) Å, V = 9213(4) Å^3, $\rho_{calcd.}$ = 1.292 g cm^{-3}, T = 293 K, 2θ range = 2.4−54.0°, 25 reflections used for cell parameter refinement, scan speed 4.0−60.0° min^{-1}, 7672 measured reflections, 7198 unique reflections, 3637 observed reflections [$I > 2\,\sigma(I)$], 531 parameters, R_1 = 0.07, $R_w(F^2)$ = 0.224. Further details of the crystal structure determination may be obtained from the Fachinformationszentrum Karlsruhe, D-76344 Eggenstein-Leopoldshafen (Germany), on quoting the depository number CSD-410110.

2a−e · (BF_4): (a) Reduction with cobaltocene: To a dark green solution of the complexes **1a−e** · $(BF_4)_2$ in 20 mL of CH_2Cl_2 [**1a** · $(BF_4)_2$: 8.4 mg; **1b** · $(BF_4)_2$: 8.7 mg; **1c** · $(BF_4)_2$: 9.2 mg; **1d** · $(BF_4)_2$: 9.7 mg; **1e** · $(BF_4)_2$: 8.5 mg; 5 × 10^{-3} mmol] were added 0.5 mL of a Cp_2Co solution (10^{-2} M in CH_2Cl_2). The colour changed to bright blue. This solution was analysed by UV/Vis and EPR spectroscopy. For the low-temperature EPR measurements a mixture of 14 mL of THF and 6 mL of CH_2Cl_2 was used instead of 20 mL of CH_2Cl_2. − (b) Reduction with sodium isopropoxide: To a dark green solution of the complexes **1a−e** · $(BF_4)_2$ in 30 mL of CH_2Cl_2/10 mL of iPrOH [**1a** · $(BF_4)_2$: 16.8 mg; **1b** · $(BF_4)_2$: 17.4 mg; **1c** · $(BF_4)_2$: 18.4 mg; **1d** · $(BF_4)_2$: 19.4 mg; **1e** · $(BF_4)_2$: 17.0 mg; 1 × 10^{-2} mmol] was added 0.5 mL of a solution of iPrONa in CH_2Cl_2 (2 × 10^{-2} M) in 0.1-mL steps. After each addition, a UV/Vis spectrum was recorded. All attempts to isolate crystals from these solutions failed as they rapidly decompose on removing the solvent. Changing the solvents or the counter ions (BF_4^-, PF_6^-, BPh_4^-) was just as unsuccessful. − (c) Crystals of **2b$_2$** · $(CoCl_4)$: To a suspension of (triphos)CoCl (560 mg, 0.78 mmol) in THF (15 mL) was added a solution of 3,6-dichloro-2,5-dihydroxy-1,4-benzoquinone (81 mg, 0.39 mmol) in EtOH (5 mL). The (triphos)CoCl dissolved completely and the solution turned bright blue. After stirring for 30 min, the progress of the reaction was checked by UV/Vis spectroscopy and a solution of $NaBPh_4$ (133.5 mg, 0.39 mmol) in 5 mL of EtOH was added. After filtration and concentration of the solution to approximately 7−8 mL the solution was layered with Et_2O (10 mL). Bright blue crystals of **2b$_2$** · $(CoCl_4)$ suitable for X-ray-crystallographic analysis were obtained within one week.

3 · $(PF_6)_2$: A solution of $CoCl_2$ (130 mg, 1 mmol) in EtOH (15 mL) was added to a solution of the triphos ligand (624 mg, 1 mmol) in THF (15 mL). Addition of solid 2,3,6,7-tetrahydroxy-9,10-dimethylanthracene (135 mg, 0.5 mmol) resulted in a colour change to blue. After the addition of solid $NaPF_6$ (168 mg, 1 mmol), the solution was stirred for 1 h and concentrated to approximately 10 mL. The resulting precipitate was separated by filtration, washed with Et_2O (2 × 10 mL), EtOH (2 × 7 mL) and again with Et_2O (2 × 10 mL). To remove NaCl the blue powder was dissolved in CH_2Cl_2 and filtered through 2 cm of Kieselgur. Addition of Et_2O precipitated **3** · $(PF_6)_2$ in 59% yield (567 mg). − M.p. 240 °C (decomp.). − IR (CsI): $\tilde{\nu}$ = 829 (br., PF). − MS (FAB); m/z (%): 1778 (5) [M^+ + PF_6], 1632 (15) [M^+], 1027 (15) [M^+ − triphos − Co + Ph + 1], 950 (25) [M^+ − triphos − Co], 816 (10) [M^{2+}]. − UV/Vis (CH_2Cl_2): λ_{max} (ε) = 376 nm (9450 M^{-1} cm^{-1}), 404 (6360, sh), 610 (3540), 909 (19140), 1250 (1440, sh). − CV (CH_3CN): $E_{1/2}$ = −0.170 V (rev.), −0.355 V (rev.), +0.335 V (rev.), E_p = +0.935 (irr.). − ^{1}H NMR (CD_2Cl_2): 1.75 (br. s, 3 H, triphos-CH_3), 2.63 (br. s, 6 H, triphos-CH_2), 3.10 (s, 3 H, ligand-CH_3), 7.0−7.5 (m, 30 H, triphos-CH_{ar}), 9.2 (s, 2 H, ligand-CH). − ^{31}P NMR (CD_2Cl_2): 31.1 (s, 3 P, triphos-P), −144.2 (sept., 1 P, PF_6, $^1J_{PF}$ = 713 Hz). − $C_{98}H_{88}Co_2F_{12}O_4P_8$ (1922.3): calcd. for **3** · $(PF_6)_2$ · 0.5 · CH_2Cl_2 C 60.18, H 4.56; found C 60.06, H 5.04.

Reduction of 3 · $(PF_6)_2$ with Cobaltocene to Obtain 4 · (PF_6): To a blue solution of **3** · $(PF_6)_2$ (9.6 mg; 5 × 10^{-3} mmol) in CH_2Cl_2 (20 mL) was added 0.5 mL of a Cp_2Co solution (10^{-2} M in CH_2Cl_2). The colour changed to orange-brown. This solution was analysed by UV/Vis and EPR spectroscopy. Addition of a second equivalent of the Cp_2Co solution (0.5 mL) resulted in a colour change to yellow.

Oxidation of 3 · $(PF_6)_2$ with Ferrocenium Tetrafluoroborate to Obtain 5^{3+}: To a blue solution of **3** · $(PF_6)_2$ (9.6 mg; 5 × 10^{-3} mmol) in CH_2Cl_2 (20 mL) was added 0.5 mL of a $[Cp_2Fe](BF_4)$ solution (10^{-2} M in CH_2Cl_2). The colour changed to green. This solution was analysed by UV/Vis and EPR spectroscopy.

Acknowledgments

This work received support from the Deutsche Forschungsgemeinschaft, the Fonds der Chemischen Industrie and the Volkswagenstiftung.

[1] K. Heinze, S. Mann, G. Huttner, L. Zsolnai, *Chem. Ber.* **1996**, *129*, 1115−1122.
[2] K. Heinze, G. Huttner, P. Schober, *Eur. J. Inorg. Chem.* **1998**, 183−189.

[3] K. Heinze, G. Huttner, L. Zsolnai, A. Jacobi, P. Schober, *Chem. Eur. J.* **1997**, *3*, 732−743.
[4] L. Sacconi, F. Mani, *Transition Met. Chem. (N. Y.)* **1982**, *8*, 179−252, and references cited therein.
[5] R. Morassi, I. Bertini, L. Sacconi, *Coord. Chem. Rev.* **1973**, *11*, 343−402, and references cited therein.
[6] S. Beyreuther, J. Hunger, G. Huttner, S. Mann, L. Zsolnai, *Chem. Ber.* **1996**, *129*, 745−757.
[7] C. Mealli, S. Midollini, L. Sacconi, *Inorg. Chem.* **1975**, *14*, 2513−2521.
[8] K. Heinze, G. Huttner, L. Zsolnai, P. Schober, *Inorg. Chem.* **1997**, *36*, 5457−5469.
[9] K. Heinze, G. Huttner, unpublished results.
[10] C. A. Ghilardi, C. Mealli, S. Midollini, V. I. Nefedov, A. Orlandini, L. Sacconi, *Inorg. Chem.* **1980**, *19*, 2454−2462.
[11] K. Heinze, G. Huttner, L. Zsolnai, *Chem. Ber.* **1997**, *130*, 1393−1403.
[12] C. Bianchini, D. Masi, C. Mealli, A. Meli, G. Martini, F. Laschi, P. Zanello, *Inorg. Chem.* **1987**, *26*, 3683−3693.
[13] V. Körner, A. Asam, G. Huttner, L. Zsolnai, M. Büchner, *Z. Naturforsch.* **1994**, *49b*, 1183−1192.
[14] C. Creutz, *Prog. Inorg. Chem.* **1983**, *30*, 1−73.
[15] N. S. Hush, *Prog. Inorg. Chem.* **1967**, *8*, 391−444.
[16] Y.-D. Gao, K. B. Lipkowitz, F. A. Schulz, *J. Am. Chem. Soc.* **1995**, *117*, 11932−11938.
[17] P. W. Crawford, F. A. Schulz, *Inorg. Chem.* **1994**, *33*, 4344−4350.
[18] M. C. Zerner, *Reviews in Computational Chemistry*, VCH, Weinheim (Germany), **1991**, p. 313−365.
[19] As the phosphorus nuclei of the PF_6^- anion have a significantly lower relaxation rate than the phosphorus nuclei bound to the cobalt centre the relaxation delay between two pulses has to be increased (see ref.[3]). The ^{31}P-NMR spectra were measured with a relaxation delay time of 2.5 s.
[20] M. B. Robin, P. Day, *Adv. Inorg. Chem. Radiochem.* **1967**, *10*, 247−269.
[21] A. Muth, Diplomarbeit, University of Heidelberg, **1989**.
[22] P. Boldt, *Chem. Ber.* **1967**, *100*, 1270−1280.
[23] L. Sacconi, S. Midollini, *J. Chem. Soc., Dalton Trans.* **1972**, 1213−1216.
[24] J. Ellermann, J. F. Schindler, *Chem. Ber.* **1976**, *109*, 1095−1105.
[25] [25a] G. M. Sheldrick, *SHELXS 86*, *Program for Crystal Structure Solution*, University of Göttingen, **1986**. − [25b] G. M. Sheldrick, *SHELXL 93*, *Program for Crystal Structure Refinement*, University of Göttingen, **1993**.
[26] L. Zsolnai, G. Huttner, *XPMA*, *ZORTEP*, University of Heidelberg, **1998**; http://www.rzuser.uni-heidelberg.de/v54.xpm.html

Received September 23, 1998
[I98329]